International Journal for Parasitology 54 (2024) 391–400

Contents lists available at ScienceDirect

International Journal for Parasitology

journal homepage: www.elsevier.com/locate/ijpara

Intricate balance of dually-localized catalase modulates infectivity of *Leptomonas seymouri* (Kinetoplastea: Trypanosomatidae)

L'ubomíra Chmelová [a,1], Natalya Kraeva [a,1], Andreu Saura [a], Adam Krayzel [a], Cecilia Stahl Vieira [b,2], Tainá Neves Ferreira [b], Rodrigo Pedro Soares [c], Barbora Bučková [d], Arnau Galan [a], Eva Horáková [e,3], Barbora Vojtková [f], Jovana Sádlová [f], Marina N. Malysheva [g], Anzhelika Butenko [a,e,h], Galina Prokopchuk [e,h], Alexander O. Frolov [g], Julius Lukeš [e,h], Anton Horváth [d], Ingrid Škodová-Sveráková [a,d,e], Denise Feder [b,i,j], Alexei Yu. Kostygov [a,g], Vyacheslav Yurchenko [a,*]

[a] *Life Science Research Centre, Faculty of Science, University of Ostrava, Ostrava, Czechia*
[b] *Universidade Federal Fluminense, Instituto de Biologia, Programa de Pós-Graduação em Ciências e Biotecnologia, Niterói, Brazil*
[c] *Biotechnology Applied to Pathogens (BAP), Instituto René Rachou, Fundação Oswaldo Cruz, Belo Horizonte, Brazil*
[d] *Department of Biochemistry, Faculty of Natural Sciences, Comenius University, Bratislava, Slovakia*
[e] *Institute of Parasitology, Biology Centre, Czech Academy of Sciences, České Budějovice, Czechia*
[f] *Department of Parasitology, Faculty of Science, Charles University, Prague, Czechia*
[g] *Zoological Institute, Russian Academy of Sciences, St. Petersburg, Russia*
[h] *Faculty of Science, University of South Bohemia, České Budějovice, Czechia*
[i] *Universidade Federal Fluminense, Instituto de Biologia, Laboratório de Biologia de Insetos, Niterói, Brazil*
[j] *Instituto Nacional de Entomologia Molecular, Rio de Janeiro, Brazil*

ARTICLE INFO

Article history:
Received 5 December 2023
Received in revised form 24 March 2024
Accepted 19 April 2024
Available online 23 April 2024

Keywords:
Trypanosomatids
Hydrogen peroxide
Catalase

ABSTRACT

Nearly all aerobic organisms are equipped with catalases, powerful enzymes scavenging hydrogen peroxide and facilitating defense against harmful reactive oxygen species. In trypanosomatids, this enzyme was not present in the common ancestor, yet it had been independently acquired by different lineages of monoxenous trypanosomatids from different bacteria at least three times. This observation posited an obvious question: why was catalase so "sought after" if many trypanosomatid groups do just fine without it? In this work, we analyzed subcellular localization and function of catalase in *Leptomonas seymouri*. We demonstrated that this enzyme is present in the cytoplasm and a subset of glycosomes, and that its cytoplasmic retention is H_2O_2-dependent. The ablation of catalase in this parasite is not detrimental in vivo, while its overexpression resulted in a substantially higher parasite load in the experimental infection of *Dysdercus peruvianus*. We propose that the capacity of studied flagellates to modulate the catalase activity in the midgut of its insect host facilitates their development and protects them from oxidative damage at elevated temperatures.

1. Introduction

Hydrogen peroxide (H_2O_2) is both an oxidizing and a reducing agent. This is explained by the fact that its two atoms of oxygen have the oxidation state of −1 in contrast to the most frequent 0 or −2 states in other compounds. Hydrogen peroxide emerges in cells either as a by-product of aerobic metabolism or, as a small uncharged molecule, it can penetrate biological membranes via peroxiporins from the environment (González-Flecha and Demple, 1995; Bienert et al., 2007; Ouchi et al., 2019). Its accumulation inside the cell must be strictly controlled because, on the one hand, it serves as a redox signaling molecule, while on the other hand, it can be decomposed to the extremely reactive and toxic hydroxyl radical (OH·) (Rhee, 1999; Brand, 2016).

Nearly all aerobic organisms are equipped with catalases, powerful enzymes scavenging hydrogen peroxide (Percy, 1984; Zámocký et al., 2008). Most of these proteins function as homotetramers with one Fe^{III} heme *b* group per subunit (Zámocký and Koller, 1999; Díaz et al., 2012). Catalase decomposes H_2O_2 into

* Corresponding author.
E-mail address: vyacheslav.yurchenko@osu.cz (V. Yurchenko).
[1] These authors contributed equally.
[2] Current address: Department of Parasitology, Faculty of Science, Charles University, Prague, Czechia.
[3] Current address: Institute of Microbiology, Czech Academy of Sciences, Třeboň, Czechia.

https://doi.org/10.1016/j.ijpara.2024.04.007
0020-7519/

molecular oxygen and water in a two-step reaction. In the first step, a ferric cation Fe^{III} reacts with H_2O_2 producing an oxidized Fe^{IV} form of an oxoferryl π-cation radical and water. In the second step, another molecule of H_2O_2 acts as an electron donor and Fe^{IV} is reduced to its initial stage, followed by the production of molecular oxygen and the second molecule of water (Nicholls et al., 2000).

When a host cell becomes infected by a pathogen, rapid generation of reactive oxygen species (ROS), exemplified by the membrane-permeable and highly reactive hydroxyl radicals as by-products of H_2O_2 decomposition, are indispensable for cellular defense (Diaz-Albiter et al., 2012; Bahia et al., 2013; Nogueira et al., 2015; Dumas and Knaus, 2021). To neutralize hydroxyl radicals, many pathogens utilize enzymes, among which catalase is a key component of the detoxification pathway, allowing survival in such adverse conditions. While this role of catalase has been well documented in bacteria (Mandell, 1975; Manca et al., 1999; Lefebre and Valvano, 2001), the situation appears to be more complex in protistan parasites. Indeed, *Toxoplasma gondii* relies on catalase for defense against the oxidative stress imposed by the host (Ding et al., 2004), yet other parasites such as *Plasmodium*, *Babesia*, *Leishmania*, and *Trypanosoma* spp. lack this seemingly ubiquitous enzyme (Kraeva et al., 2017). Hence, the mechanisms by which they evade the typical host-derived respiratory burst remain poorly understood.

Arguably, the most prominent example of complex catalase distribution is the family Trypanosomatidae (Euglenozoa: Kinetoplastea) (Kostygov et al., 2024). These highly divergent omnipresent parasites infect insects, leeches, vertebrates, and plants (Lukeš et al., 2018; Frolov et al., 2021). The evolutionary history of catalase in trypanosomatids is unexpectedly complex (Škodová-Sverá ková et al., 2020), as the enzyme is absent from other kinetoplastids, implying that their common ancestor lacked it (Opperdoes et al., 2016). Hence, the genes encoding this enzyme must have been independently acquired by different lineages of monoxenous (with one host in the life cycle) trypanosomatids from different bacteria at least three times (Chmelová et al., 2021). This observation posited an obvious question: why was catalase so "sought after" if many trypanosomatid groups do just fine without it? One of the approaches to tackle this question was to express catalase in flagellates, which do not possess it. In *Trypanosoma cruzi*, the overexpression of catalase enhanced the parasite's proliferation in the insect vector, impaired stress-mediated signaling, but did not affect parasitemia in mice (Freire et al., 2017). However, in *Trypanosoma brucei* and *Leishmania mexicana*, the development in both insect and vertebrate hosts was impaired upon catalase expression (Horáková et al., 2020; Sádlová et al., 2021). Out of the three model species mentioned above, the most intriguing one seems to be *L. mexicana*. It belongs to the subfamily Leishmaniinae (Kostygov and Yurchenko, 2017), whose common ancestor acquired catalase. The gene encoding catalase was retained in the monoxenous members of this subfamily, but secondarily lost in *Leishmania* sensu lato, which switched to dixeny (life cycle with two hosts) (Kraeva et al., 2017). A somewhat circumstantial explanation for this prominent loss may lay in the fact that H_2O_2 was shown to act as a signaling molecule facilitating *Leishmania* differentiation and virulence (Mittra et al., 2013; Khan et al., 2018; Xiang et al., 2019). Moreover, catalase of Leishmaniinae contains an eight amino acid "catalase-related immune-responsive" domain, which triggers a T cell-mediated immune response (Guy et al., 2005; Hewitt and Degnan, 2023). Thus, loss of a catalase might have been an event facilitating later adaptation to the vertebrate hosts.

The sub-cellular localization of catalase in eukaryotes remains debated. An early work in the trypanosomatid *Crithidia fasciculata* reported catalase activity in the cytoplasmic fraction (Edwards and Lloyd, 1977), while a later study on a related flagellate, *Leptomonas* (now *Herpetomonas*) *samueli*, documented its association with the glycosomes (Souto-Padrón and de Souza, 1982), organelles homologous to peroxisomes of other organisms (Opperdoes and Michels, 1993; Michels and Gualdrón-López, 2022). Due to the presence of peroxisomal targeting signal(s) (PTS), catalase in most eukaryotes is considered a peroxisomal enzyme (Gould et al., 1989), which correlates nicely with the posited glycosomal localization in trypanosomatids. In humans, the C-terminal PTS of catalase is recognized by the cytosolic receptor Pex5p that facilitates its import into the peroxisomes (Otera and Fujiki, 2012), although it may also be retained in the cytoplasm upon oxidative damage induced by ROS (Dubreuil et al., 2020; Fujiki and Bassik, 2021). Moreover, the cytosolic localization of catalase was demonstrated in *T. gondii* (Ding et al., 2004), *Chlamydomonas reinhardtii* (Kato et al., 2021), and *Caenorhabditis elegans* (Taub et al., 1999). Notably, the catalases of trypanosomatids lack the PTS (Chmelová et al., 2021).

To further dissect the role(s) of catalase in trypanosomatids, we decided to investigate its function in *Leptomonas seymouri*, a monoxenous parasite that is often found in coinfections with *Leishmania* in the immunocompromised patients (Ghosh et al., 2012; Thakur et al., 2020). This species is predisposed to the dixenous life style due to its ability to withstand elevated temperatures (Kraeva et al., 2015) and, thus, represents a suitable model for a thorough characterization of this intriguing enzyme in the family Trypanosomatidae.

2. Materials and methods

2.1. Cultivation and growth kinetics

Leptomonas seymouri (isolate ATCC 30220) was maintained in either M199 (Biowest, Nuaillé, France) supplemented with 2 μg/ml of biopterin (Cayman Chemical, Ann Arbor, USA), 2 μg/ml of hemin (Merck, Rahway, USA), 25 mM HEPES, 50 units/ml of penicillin, 50 μg/ml of streptomycin (all Biowest) and 10% heat-inactivated fetal bovine serum (hiFBS) (Biosera, Cholet, France) or Schneider *Drosophila* medium (Thermo Fisher Scientific, Waltham, USA) supplemented with 10% hiFBS, 50 units/ml of penicillin, 50 μg/ml of streptomycin, and 10 μg/ml of hemin (Jena Bioscience, Jena, Germany) at 23 °C. The species identity was confirmed as in Yurchenko et al. (2016). For experiments at the elevated temperature (35 °C), all cultures were adapted to modified conditions for at least three passages before measurements. Growth kinetics was assessed for 7 days from the starting density of 5×10^5 cells/ml. Cell numbers were counted every 24 h in three biological replicates as in Ishemgulova et al. (2017). Comparison of growth curves was performed by computing areas below them using Simpson approximation in SciPy v. 1.7.3. (Virtanen et al., 2020). Normality of data distribution was assessed by a Shapiro-Wilk test and pairwise comparisons were performed using the unpaired *t*-test. The *P*-values were adjusted using Bonferroni correction. All the statistical analyses were performed in GraphPad Prism v. 9 (GraphPad Software, San Diego, USA).

2.2. Establishment of the CRISPR/Cas9 system in L. seymouri

The previously reported CRISPR/Cas9-based strategy developed in *L. mexicana* (Beneke and Gluenz, 2019) was applied to *L. seymouri*. In short, 1×10^7 cells from the early exponential phase of growth were transfected with the pTB007 plasmid (Beneke et al., 2017) using Amaxa Nucleofector IIb (Lonza, Basel, Switzerland) program X-001 and Tb-BSF buffer (90 mM sodium phosphate, 5 mM potassium chloride, 0.15 mM calcium chloride, 50 mM HEPES, pH 7.3) (Burkard et al., 2007). The resulting transfectants were selected with 200 μg/ml of hygromycin (VWR/ Avantor,

Radnor, USA), and clonal lines were isolated on solid complete M199 medium as in Hamilton et al. (2015). The expression of Cas9 and T7 RNA polymerase was confirmed by diagnostic PCR, reverse transcription-quantitative PCR (RT-qPCR) using the 18S rRNA locus for normalization (Supplementary Table S1), and by western blotting with mouse monoclonal anti-FLAG M2 antibody (Sigma-Aldrich/ Merck, Darmstadt, Germany) diluted 1:1,000 and mouse monoclonal anti-α-tubulin antibody (Sigma-Aldrich/ Merck) diluted 1:10,000 for loading control as in Kraeva et al. (2014).

2.3. Ablation, add-back, and endogenous tagging of catalase

For the generation of catalase knock-out cell lines, the donor template and guide (g)RNAs were amplified by PCR as described previously (Beneke and Gluenz, 2019) (Supplementary Table S1). Transfectants were selected with 100 μg/ml of hygromycin and 50 μg/ml of G418 (geneticin) antibiotics (Thermo Fisher Scientific). A clonal cell line (hereafter designated as KO) was established and used in all downstream experiments. Deletion of the gene was confirmed by PCR and Southern blotting (Supplementary Table S1). The lack of enzymatic activity was also confirmed by the direct catalase test as described in Sádlová et al. (2021).

The catalase add-back (hereafter designated as AB) was prepared by integration of the *L. seymouri* catalase into the 18S rRNA locus on the KO background. For that, the gene of interest was PCR-amplified and cloned into pLEXSY-sat2 (Jena Bioscience) using *Nco*I and *Not*I restriction enzymes (Supplementary Table S1). The resultant plasmid was linearized with *Swa*I prior to transfection as described elsewhere (Ishemgulova et al., 2017). The AB clonal cell line was grown on the solid complete M199 medium supplemented with 100 μg/ml of hygromycin, 50 μg/ml of G418, and 100 μg/ml of streptothricin acetyltransferase (SAT) (Jena Bioscience) antibiotics. The correct integration was confirmed by diagnostic PCR (Supplementary Table S1). The expression of the add-back gene on the RNA and protein levels was confirmed by RT-qPCR using a 60S ribosomal protein L7a-encoding *Lsey_1065_0010* (ortholog of *Lmex.07.0510*) for normalization (Ishemgulova et al., 2016) and the direct catalase test as described above.

For endogenous tagging, the N-terminal HA-V5 tag of the plasmid pVY149 (GenBank accession number **OR805450**) was substituted by HA_3 via *Bsr*GI-*Bgl*II swap. The modified sequences (HA_3, GS linker, untranslated region (UTR)) were PCR amplified (Supplementary Table S1) and fused together as in Merritt and Stuart (2013). The sequence of the resultant plasmid was submitted to GenBank under the accession number **OR519720**.

2.4. Southern blotting

Probes annealing to the gene of interest open reading frame (ORF), 3′ UTR, and neomycin resistance gene, were amplified by PCR (Supplementary Table S1) using the PCR digoxigenin probe synthesis kit (Roche Life Science, Basel, Switzerland). For Southern blotting, 30 μg of genomic DNA was digested with *Nco*I and *Eco*RV, separated on a 0.75% agarose gel, probed and processed as described previously (Ishemgulova et al., 2018; Kraeva et al., 2019).

2.5. Vectors for episomal enhanced (e)GFP expression

The vectors for episomal eGFP expression were constructed by replacing *Cas9* gene in the pTCas9 plasmid (Sollelis et al., 2015) with *eGFP* after digestion with *Hpa*I and *Pme*I. The eGFP fragments were PCR generated using pTUBneoF4rev (Kushnir et al., 2005) as a template and primers that included sequences coding for the additional C-terminal peptides (Supplementary Table S1). Transfected *L. seymouri* cells were selected with 200 μg/ml of hygromycin.

2.6. Digitonin permeabilization of untreated and H_2O_2-treated cells

Fifty million *L. seymouri* cells were washed twice in the ice-cold PBS and resuspended in the STE buffer (25 mM Tris-HCl pH 7.9, 1 mM EDTA, 250 mM sucrose) supplemented with 150 mM NaCl and complete mini EDTA-free protease inhibitor cocktail (Roche Life Science). The protein concentration was measured using a Pierce BCA protein assay kit (Thermo Fisher Scientific). Cell aliquots were subsequently incubated with increasing concentrations of digitonin (PanReac AppliChem ITW, Darmstadt, Germany) for 4 min at room temperature followed by centrifugation at 16,000 *g* for 5 min. Supernatants were analyzed by western blotting with mouse monoclonal anti-hemagglutinin (anti-HA) antibody (Sigma-Aldrich/ Merck) diluted 1:1,000, rabbit polyclonal anti-enolase antibody at 1:5,000 (Verplaetse et al., 2009), anti-triosephosphate isomerase (anti-TIM) antibody at 1:1,000, and anti-BiP (major endoplasmic reticulum (ER) chaperone binding of immunoglobulin heavy chain protein) antibody at 1:1,000. The same number of cells was incubated with 200 μM H_2O_2 (Sigma-Aldrich/ Merck) for 30 min as described previously (Okumoto et al., 2020) at 23 °C and 35 °C and processed as above using Tubulin as a loading control.

2.7. Cell viability assay

The cytotoxic effect of hydrogen peroxide was assayed by conversion of resazurin (alamarBlue, Thermo Fisher Scientific) to resorufin (Mikus and Steverding, 2000). In brief, 1×10^6 *L. seymouri* cells were treated with serial dilutions of H_2O_2 (from 64 mM to 62.5 μM at 23 °C and from 256 mM to 250 μM at 35 °C) for 1 h followed by incubation with alamarBlue (final concentration 50 μM) for 24 h. The readouts at 570 nm (reduced alamarBlue) and 600 nm (oxidized alamarBlue) were taken on Infinite 200 Pro M Nano (Tecan, Männedorf, Switzerland) and analyzed using GraphPad Prism v. 9 (GraphPad Software) by non-linear regression with variable slope to obtain half maximal inhibitory concentration (IC_{50}) values. All experiments were performed in three biological and three technical replicates in the absence or presence of H_2O_2. In the latter case, the concentrations were 0.865 mM for 23 °C and 1.29 mM for 35 °C (halves of the lowest IC_{50} values at a given temperature). Obtained IC_{50} values were tested for normal distribution using a Shapiro-Wilk test and pairwise comparisons were performed using the unpaired *t*-test.

2.8. Measurements of cellular ROS

To estimate the level of total ROS in *L. seymouri* wild-type (WT), knock-out (KO), and add-back (AB) cell lines, 5 × 10 8 cells in exponential phase of growth were harvested and incubated in fresh growth medium supplemented with 10 μg/ml of dichlorodihydrofluorescein diacetate (Sigma-Aldrich/ Merck). This cell-permeable non-fluorescent probe turns into the highly fluorescent 2′,7′-dichlorofluorescein upon oxidation. After 1 h of incubation at 23 °C or 35 °C, the cells were examined with a ZEISS fluorescence microscope (Carl Zeiss Microscopy, Oberkochen, Germany) and the fluorescence intensity was evaluated using ImageJ Fiji v. 2.14.0 (Schindelin et al., 2012) by selecting one cell at a time and measuring its area and integrated intensity. Data values were calculated for 100 examined cells per each sample and condition. The background readings were sampled and averaged from five measurements for each image. The correlated total cell density was calculated as integrated density − (area × mean fluorescence of the background readings). The obtained data were tested for normality

of distribution by the D'Agostino-Pearson K^2 test. The statistical analysis was done using the Mann-Whitney test.

2.9. Immunofluorescence microscopy and transmission electron microscopy (TEM)

Cells were fixed with 4% paraformaldehyde on glass slides, permeabilized with 1% NP-40, and blocked with 1% BSA. Next, they were incubated with mouse monoclonal anti-HA (Sigma-Aldrich/Merck) and rabbit polyclonal anti-aldolase or anti-MVAK (phosphomevalonate kinase) antibodies (both at 1:1,000) and visualized with Cy3-conjugated goat anti-rabbit IgG (Millipore/ Merck, Burlington, USA) and Alexa Fluor488-labeled goat anti-mouse IgG (Thermo Fisher Scientific) antibodies (both at 1:5,000). The nucleus and kinetoplast DNAs were stained with DAPI (Sigma-Aldrich/Merck) as described previously (Yurchenko et al., 2014). Images were acquired on Olympus BX53 fluorescent microscope (Olympus, Tokyo, Japan) equipped with the Olympus DP72 camera and processed in ImageJ Fiji v. 2.14.0. High-pressure freezing in anhydrous acetone with 2% osmium tetroxide and TEM using a JEM-1400 transmission electron microscope (JEOL, Tokyo, Japan) were performed as described previously (Yurchenko et al., 2014).

2.10. High resolution respirometry

The oxygen production of 1×10^6 cells was triggered by the addition of 0.09% H_2O_2 and monitored for 5 min using the Oroboros O2k oxygraph (Oroboros Instruments, Innsbruck, Austria) calibrated with the growth medium. The catalase activity was measured as the increase in oxygen concentration (pM) per cell per second. All experiments were performed in two biological and 4–6 technical replicates. The data were analyzed using GraphPad Prism v. 9.

2.11. Experimental infection in the insect host

Insects of the *Dysdercus peruvianus* colony established at the Laboratory of Insect Biology, Universidade Federal Fluminense, Brazil were reared in glass pots with water and cotton seeds and maintained under controlled conditions of 25 °C, 75% relative humidity, and 16:8h light:dark cycle. Fifth instar nymphs were randomly chosen and maintained as above until they molted into adults. Before the experimental infection, the insects were deprived of water and food for 24 h. For the infection, pieces of cotton soaked in a culture of *L. seymouri* (WT, KO, or AB) at the concentration of 1×10^6 parasites/ml (or water for the control) were placed in glass containers with 30 specimens each. There were two containers for each of the three experimental groups. On days 1, 7, and 10 after infection, 10 insect specimens per group were dissected and the parasite load was estimated by direct counting under a light contrast microscope. The data were analyzed using GraphPad Prism v. 9.

3. Results

3.1. Leptomonas seymouri is amenable to genetic manipulation

In the first step, we episomally expressed Cas9 nuclease and T7 RNA polymerase employing the approach that was successfully used in *Leishmania mexicana* (Beneke et al., 2017, 2019). The resultant four clonal lines (labeled Cl1-4) were tested by diagnostic PCR for the plasmid presence (Supplementary Fig. S1A), RT-qPCR for the mRNA levels of Cas9 and T7 RNA polymerase (Supplementary Fig. S1B), and western blotting for the protein level of Cas9-FLAG (Supplementary Fig. S1C). The clonal cell line 4 was chosen for all subsequent experiments.

Next, we applied the established CRISPR/Cas9 system to endogenously tag N-termini of both alleles of catalase with HA_3 (Supplementary Fig. S2A). N-terminal tagging was chosen because of the putative localization-determining amino acids presence at the other end of the catalase (see below). We confirmed expression of the tagged catalase by western blotting (Supplementary Fig. S2B) and its enzymatic activity by the direct catalase test (Supplementary Fig. S2C) using the WT strain of *L. seymouri* as negative (for western blotting) and positive (for direct catalase test) controls. Out of the three tested populations (labeled Pop1-3), population 2 was cloned out and a representative clone was used in all subsequent experiments.

3.2. Dual localization of catalase is sensitive to H_2O_2 treatment

Using a cell line with the endogenously tagged catalase, we explored its localization by immunofluorescent microscopy. Under normal conditions, the enzyme has a dual localization, being diffusely distributed in the cytoplasm and concentrated in a presumably membranous compartment in front of the nucleus and close to the kinetoplast. The compartment in question did not co-localize with aldolase, a bona fide glycosomal marker, representing an enzyme involved in both glycolysis and gluconeogenesis in trypanosomatids (Hart et al., 1987; Kovářová et al., 2018) (Fig. 1A). This pattern notably resembled the subcellular localization of catalase in *T. gondii* (Kaasch and Joiner, 2000). Since glycosomes of trypanosomatids are known to be heterogeneous (Crowe and Morris, 2021), we also investigated co-localization of catalase with another glycosomal marker, phosphomevalonate kinase (MVAK), an enzyme of the isoprenoid biosynthesis pathway (Carrero-Lérida et al., 2009) (Fig. 1B). The colocalization of MVAK and catalase suggests that the latter is confined to a subset glycosomes, which are not involved in glycolysis. Ultrastructural analysis revealed an accumulation of round and elongated glycosomes in the anterior region of the cell (Supplementary Fig. S3) further supporting the fluorescent microscopy data. We did not observe unusual or unidentified organelles in the cells.

To complement our localization data, we employed one more technique, namely digitonin permeabilization (Kiaira and Njogu, 1983; Vercesi et al., 1991), followed by western blotting analysis with antibodies against enolase (a cytoplasmic marker), triosephosphate isomerase TIM (a glycosomal marker), and a major endoplasmic reticulum (ER) chaperone binding of immunoglobulin heavy chain protein (BiP, an ER marker) (Swinkels et al., 1986; Wang et al., 2010; Škodová et al., 2013). Confirming previous results, we documented low abundance of catalase in the cytoplasmic fraction, while most of the signal was associated with a membranous compartment of the sterol composition reminiscent of the glycosomes (Fig. 2A). Prompted by recent intriguing observation that in the mammalian cells H_2O_2 suppresses the import of catalase into the peroxisomes, leading to the spatiotemporal increase of its concentration in the cytoplasm to counteract ROS (Okumoto et al., 2020), we investigated this phenomenon in *L. seymouri*. Indeed, the treatment with H_2O_2 resulted in an increased level of catalase in the cytoplasm (Fig. 2B), while the total amount of the enzyme was not affected at either low or elevated temperature (Fig. 2C), further confirming that its dual localization and cytoplasmic abundance are H_2O_2-dependent.

The catalases of monoxenous trypanosomatids lack canonical peroxisomal targeting signals PTS1 or PTS2 (Chmelová et al., 2021). However, the studied enzyme of *L. seymouri* bears an additional Trp-Pro dipeptide on its very C-terminus (Supplementary Fig. S4A). To address the question of whether this motif determines catalase localization, we exogenously expressed eGFP with C-terminal extensions of *L. seymouri* (−SEAEIWP), *Leptomonas pyrrhocoris* (−SEAEI), and a canonical PTS1 (−AKL). As expected, eGFP-AKL localized to the glycosomes, while eGFP, eGFP-SEAEI,

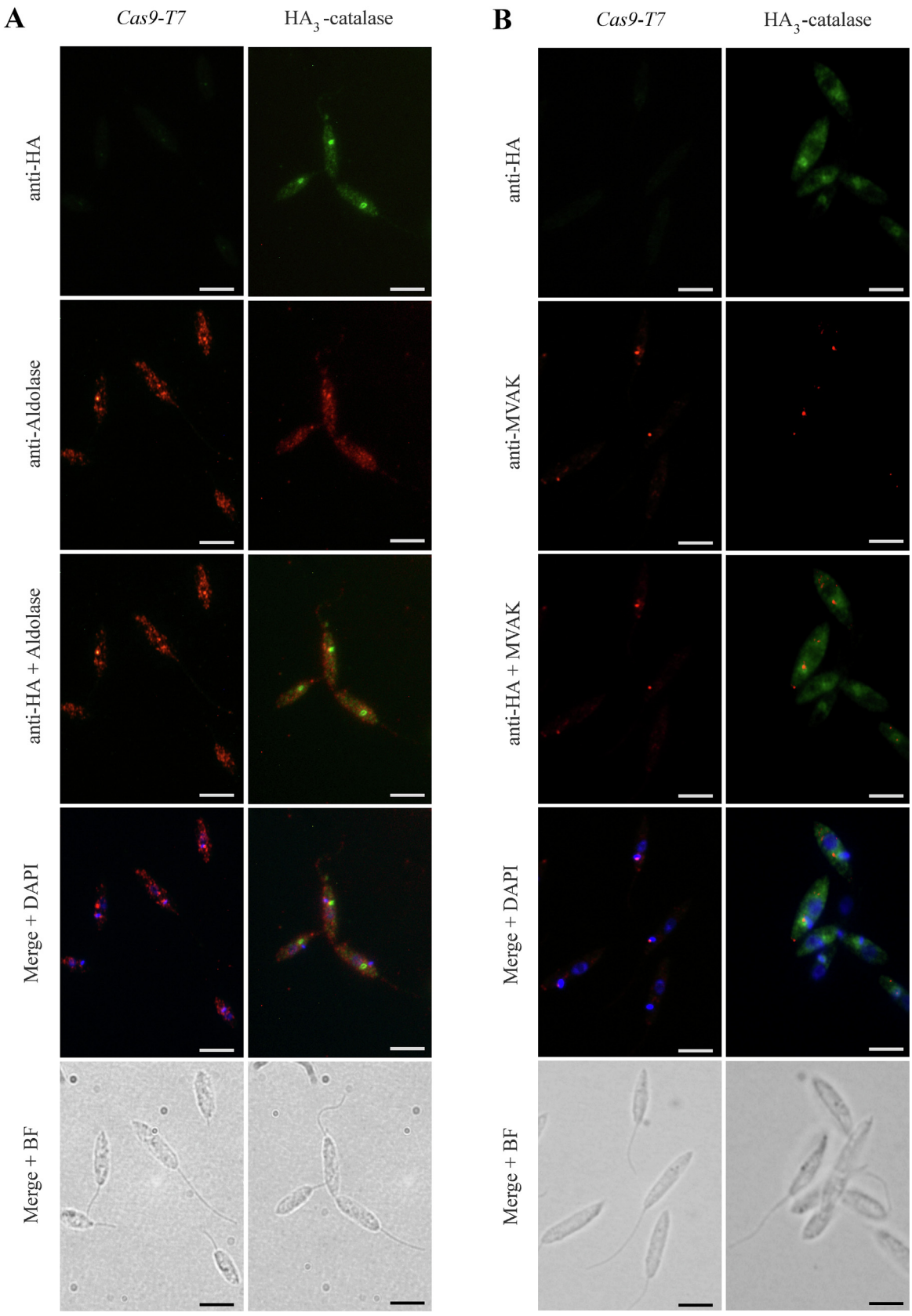

Fig. 1. Localization of *Leptomonas seymouri* catalase analyzed by microscopy. Immunofluorescence analysis of N-terminally hemagglutinin (HA)-tagged *L. seymouri* catalase (green). Co-stainings with anti-aldolase (A, red) and anti- phosphomevalonate kinase MVAK (B, red) antibodies were used to assess colocalization. Nuclei and kinetoplasts are stained with DAPI. BF, bright field. Scale bar = 5 μm. (For interpretation of the references to colour in this figure legend, the reader is referred to the web version of this article.)

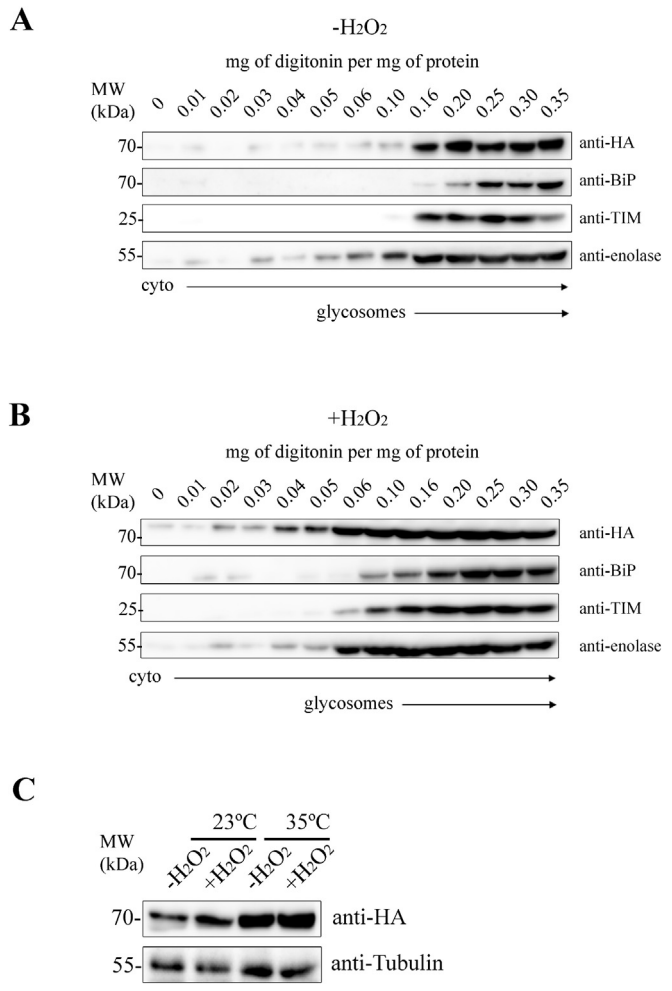

Fig. 2. Localization of *Leptomonas seymouri* catalase analyzed by the differential digitonin permeabilization method. (A, B) Hemagglutinin (HA)-tagged catalase localization after digitonin fractionation in untreated (A) and 0.2 mM hydrogen peroxide-treated (B) cultures of *L. seymouri* analyzed by western blotting with anti-HA, −BiP (major endoplasmic reticulum (ER) chaperone binding of immunoglobulin heavy chain protein), −triosephosphate isomerase (TIM), and −enolase antibodies. Molecular weights in kDa are indicated. (C) The total amount of HA-tagged catalase in treated and untreated samples at low and elevated temperatures analyzed by western blotting with anti-HA antibody. Tubulin was used as a loading control.

and eGFP-SEAEIWP were cytosolic (Supplementary Fig. S4B) proving that the C-terminal WP motif does not determine catalase localization in the studied flagellate.

3.3. Catalase is dispensable in vitro but enhances resistance to H_2O_2 when overexpressed

To further dissect the role of catalase, we ablated the corresponding gene (*Lsey_0026_0490*) using the CRISPR/Cas9 system and established the AB cell line by integrating the gene of interest into the 18S rRNA locus on the KO background (Supplementary Fig. S5). The selected AB clonal cell line had approximately twofold higher RNA level of catalase compared with the WT strain (Supplementary Fig. S5B). Importantly, estimation of the enzymatic activity showed the same difference, as the production of molecular oxygen in the WT and AB cells (with KO strain used as a negative background) amounted to 17.9 and 35.8 fmol O_2/min × cell, respectively (Supplementary Fig. S5D). This is in line with the previously reported activity of catalase in *L. pyrrhocoris* (Bianchi et al., 2019).

Comparison of the growth kinetics under different temperatures in the absence of hydrogen peroxide revealed that *L. seymouri* multiplies faster at 35 °C than at 23 °C. Moreover, AB cells divided slower, a difference that was more pronounced at 35 °C (Fig. 3A). When cultivated in the presence of hydrogen peroxide, AB cells withstood these conditions better, again showing more pronounced difference at the elevated temperature (Supplementary Fig. S6). Using the alamarBlue assay, we examined the ability of cells to withstand the cytotoxic effects of H_2O_2 (Fig. 3B). At 23 °C, the ablation of catalase had little (if any) effect, while its overexpression provided a significant survival advantage with IC_{50} values of 1.76 ± 0.15, 1.73 ± 0.15, and 4.07 ± 0.79 mM for the WT, KO, and AB cell lines. In agreement with the previously demonstrated elevation of catalase expression at 35 °C (Kraeva et al., 2015), the tolerance of WT, KO, and AB cell lines to H_2O_2 increased with the IC_{50} values of 3.42 ± 0.03 mM, 2.83 ± 0.26, and 5.71 ± 1.21 mM, respectively. At this elevated temperature, ablation and modest overexpression of catalase in the KO and AB cell lines had a negative and a positive influence on *L. seymouri* survival, respectively (Fig. 3B). This correlated well with levels of intracellular ROS measured at both temperatures (Fig. 3C), providing additional evidence to support the conclusion that catalase plays a protective role in protecting *L. seymouri* from the oxidative damage.

3.4. Catalase is dispensable in vivo but facilitates infection when overexpressed

The cotton stainer *D. peruvianus* (Hemiptera: Pyrrhocoridae) is the only host in which *L. seymouri* has been demonstrated to complete its developmental cycle (Moraes et al., 1994). This bug is closely related to *Dysdercus suturellus*, a species from which *L. seymouri* was originally isolated (Wallace, 1977). Experimental infections of the cotton stainer with the WT, KO, and AB strains of *L. seymouri* demonstrated a situation similar to that observed in vitro. Specifically, the ablation of catalase had no detectable effect on infectivity, while its overexpression resulted in a significant increase (approximately an order of magnitude on day 10) in parasite abundance (Fig. 4).

4. Discussion

Using the model of *L. seymouri*, we aimed to answer two intriguing questions about trypanosomatid catalase. The first one concerned cellular localization of this extremely potent enzyme, which was reported to be cytoplasmic in *C. fasciculata*, while confined to glycosomes in the related *Leptomonas* (now *Herpetomonas*) *samueli* (Edwards and Lloyd, 1977; Souto-Padrón and de Souza, 1982). To settle this discrepancy, we used a battery of methods to show that in yet another related flagellate, catalase is localized in both the glycosomes and cytoplasm, proving the earlier reports correct. Such a dual localization is not unprecedented, since a similar pattern was documented in *Saccharomyces cerevisiae*, *T. gondii*, and a range of other species (reviewed in Fujiki and Bassik, 2021). Of note, the localization of enzymes in two cellular compartments is not unusual in trypanosomatids, as was demonstrated for hexokinase 2 (Joice et al., 2012), lyso-phospholipase A (Monic et al., 2022), UDP-glucose pyrophosphorylase (Villafraz et al., 2021), or *iso*-citrate dehydrogenase (Pyrih et al., 2023). It remains to be established what determines the glycosomal localization of catalase in *L. seymouri*, as it lacks identifiable PTSs. Since it was previously shown that an internal import signal governs the glycosomal localization of *T. cruzi* phosphoglucomutase even in the absence of PTS1 or PTS2 (Penha et al., 2009), similar mechanisms may be in place for catalase. To complicate the picture further, our data indicate that catalase is present only in a subfraction of glycosomes,

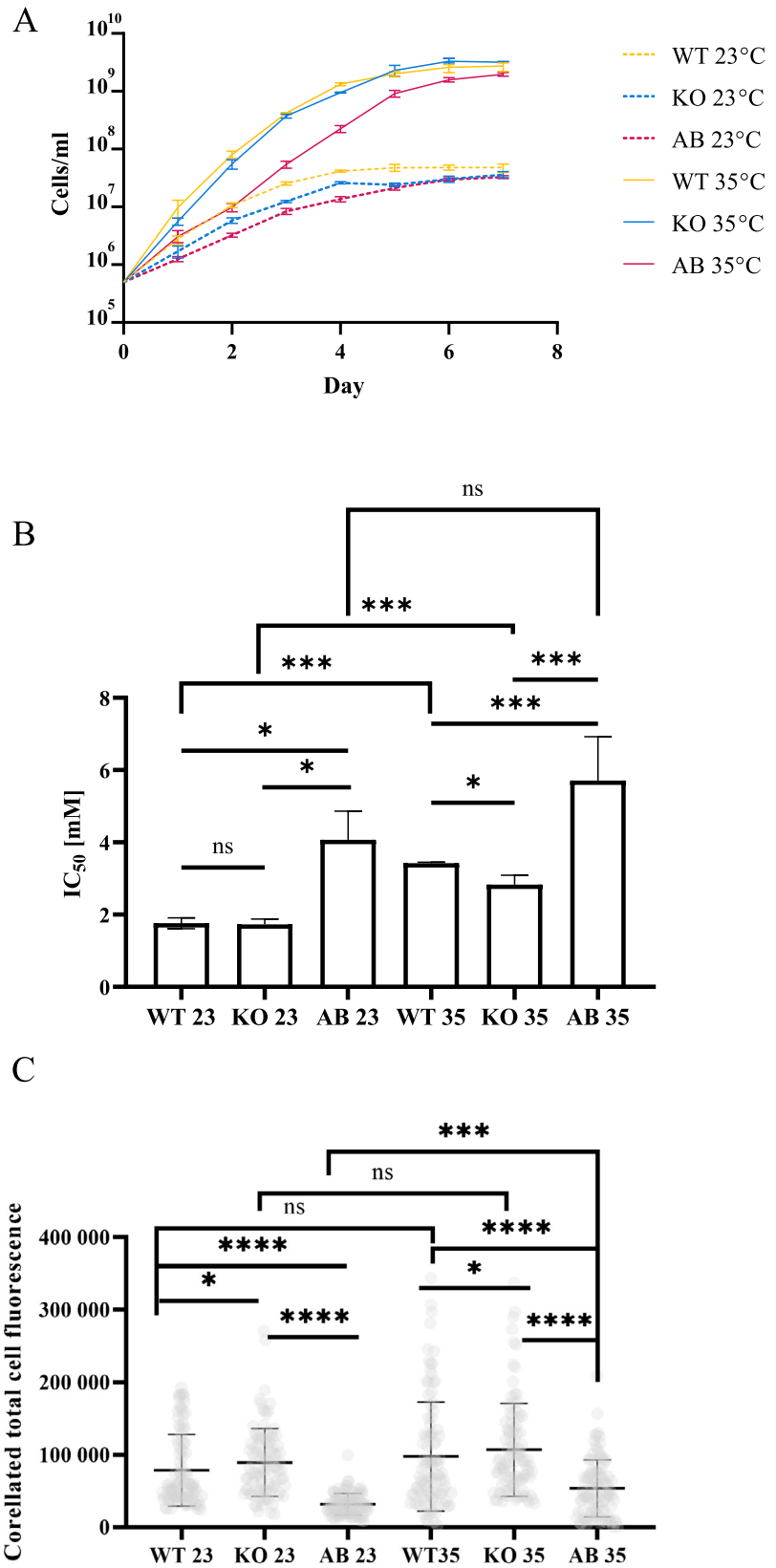

Fig. 3. The effect of catalase ablation in *Leptomonas seymouri* in vitro. (A) Comparison of growth rates of wild-type (WT), knock-out (KO), and add-back (AB) lines of *L. seymouri* at 23 °C and 35 °C. (B) Half maximal inhibitory concentration (IC_{50}) for the WT, KO, and AB *L. seymouri* at 23 °C and 35 °C. The data and statistical analyses represent three independent biological replicates. (C) Intracellular reactive oxygen species (ROS) in WT, KO, and AB *L. seymouri* cells at 23 °C and 35 °C. The error bars indicate S.D.; $^{*}P \leq 0.05$; $^{**}P \leq 0.001$; $^{***}P \leq 0.00001$; ns, not statistically significant.

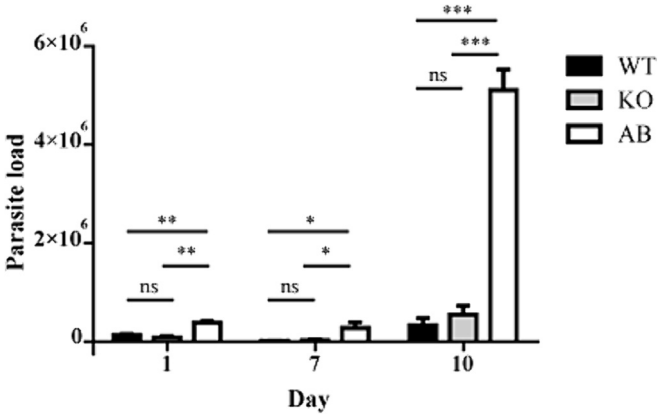

Fig. 4. Development of *Leptomonas seymouri* in experimental infection of *Dysdercus peruvianus*. Intensity of infection was assayed on days 1, 7, and 10. The error bars indicate S.D.; $^{*}P \leq 0.05$; $^{**}P \leq 0.001$; $^{***}P \leq 0.00001$; ns, not statistically significant. WT, wild-type; KO, knock-out; AB, add-back.

likely in those not involved in glycolysis. However, how such specificity would be achieved remains unclear.

In the mammalian cells, catalase was implicated in the protection against ROS because a substantial proportion of this enzyme was retained in the cytoplasm upon treatment with H_2O_2 (Okumoto et al., 2020; Fujiki and Bassik, 2021). Our observation of a very similar pattern in *L. seymouri* argues that the cytoplasmic retention of catalase is a widespread phenomenon in eukaryotes.

The second question we wanted to addressed is the function of catalase in trypanosomatids, since its absence in the serious human pathogens *Leishmania* and *Trypanosoma* spp. indirectly implied that the presence of this enzyme is incompatible with parasitism in the vertebrate hosts (Kraeva et al., 2017). However, the apparent absence of catalase in the last common ancestor of all trypanosomatids argues against this scenario (Butenko et al., 2021). It is clear that for some extant trypanosomatids the presence of catalase is useful, if not essential, as reflected by at least three independent acquisitions of the catalase-encoding genes from different bacterial linages (Chmelová et al., 2021). Given such a patchy distribution, it is not surprising that the ablation of catalase in *L. seymouri* has little effect in vitro and in vivo. This observation correlates well with the generally asymptomatic phenotype of catalase depletion in the bacteria *Escherichia coli* and *Salmonella typhimurium*, as well as in the eukaryote *S. cerevisiae* (Ma and Eaton, 1992; Buchmeier et al., 1995; Izawa et al., 1996). At the same time, its overexpression in *T. gondii* leads to an increased fitness and invasiveness (Ding et al., 2004) reminiscent of the data reported here for *L. seymouri*.

Based on the available data, especially the upregulation of catalase at elevated temperatures, we propose that catalase acts under stressful conditions and provides higher tolerance against H_2O_2. Indeed, at high temperatures, the insect host experiences oxidative stress accompanied by an increase in the levels of ROS and H_2O_2 (Zhong et al., 1998; Neven, 2000). As such, the catalase of *L. seymouri* seems to serve as an emergency enzyme needed mainly when its host becomes overheated, a situation expected to occur regularly considering that *Dysdercus* spp. live in the tropics.

In conclusion, we show that in *L. seymouri* catalase is present in the cytoplasm and a subset of glycosomes, and that its cytoplasmic retention is H_2O_2-dependent. The ablation of catalase in *L. seymouri* is not detrimental in vivo, while its overexpression resulted in a substantially higher parasite load in the experimental infection of *D. peruvianus*. We propose that the capacity of studied flagellates to modulate catalase activity in the midgut of its insect host facilitates their development and protects them from oxidative damage at elevated temperatures.

CRediT authorship contribution statement

Ľubomíra Chmelová: Data curation, Formal analysis, Investigation, Methodology, Writing – original draft, Writing – review & editing. **Natalya Kraeva:** Data curation, Formal analysis, Investigation, Supervision, Writing – original draft, Writing – review & editing. **Andreu Saura:** Data curation, Formal analysis, Writing – review & editing. **Adam Krayzel:** Investigation, Writing – review & editing. **Cecilia Stahl Vieira:** Investigation, Writing – review & editing. **Tainá Neves Ferreira:** Investigation, Writing – review & editing. **Rodrigo Pedro Soares:** Investigation, Writing – review & editing. **Barbora Bučková:** Investigation, Writing – review & editing. **Arnau Galan:** Investigation, Writing – review & editing. **Eva Horáková:** Formal analysis, Writing – review & editing. **Barbora Vojtková:** Investigation, Writing – review & editing. **Jovana Sádlová:** Investigation, Writing – review & editing. **Marina N. Malysheva:** Investigation, Writing – review & editing. **Anzhelika Butenko:** Investigation, Writing – review & editing. **Galina Prokopchuk:** Investigation, Validation, Writing – review & editing. **Alexander O. Frolov:** Investigation, Writing – original draft. **Julius Lukeš:** Formal analysis, Funding acquisition, Resources, Supervision, Validation, Writing – review & editing. **Anton Horváth:** Formal analysis, Funding acquisition, Supervision, Validation, Writing – review & editing. **Ingrid Škodová-Sveráková:** Data curation, Formal analysis, Funding acquisition, Investigation, Resources, Supervision, Writing – review & editing. **Denise Feder:** Formal analysis, Investigation, Writing – review & editing. **Alexei Yu. Kostygov:** Data curation, Formal analysis, Investigation, Validation, Visualization, Writing – review & editing. **Vyacheslav Yurchenko:** Conceptualization, Data curation, Formal analysis, Funding acquisition, Methodology, Resources, Supervision, Validation, Visualization, Writing – original draft, Writing – review & editing.

Acknowledgements

We thank Drs. J. Bangs (University of Buffalo, USA) and D. González-Pacanowska (Instituto de Parasitología y Biomedicina "López - Neyra", Spain) for providing anti-BiP and anti-MVAK antibodies, respectively, and Z. Dzureková (Comenius University, Slovakia) for assistance with ROS measurement. This work was primarily supported by the Grant Agency of Czech Republic (21-09283S to VY and JL). Additional funding was provided by the European Union Operational Program "Just Transition" (LERCO CZ.10.03.01/00/22_003/0000003 to VY), the Ministry of Education, Youth and Sports of the Czech Republic (INTER-EXCELLENCE-LUASK22033 to VY), Infravec2/Horizon2020 program (731060 to JS), and the Slovak Research and Development Agency (SK-CZ-RD-21-0038 to AH). Ľ.Ch, AK, and AG were supported by the University of Ostrava, Czechia (SGS/PrF/2024). AG was additionally suppoprted from the budget of Moravskoslezský kraj, Czechia. RPS was funded by the Conselho Nacional de Pesquisa e Desenvolvimento, Brazil (CNPq 302972/2019-6; 305238/2023-0) and Fundação de Amparo à Pesquisa do Estado de Minas Gerais, Brazil (FAPEMIG PPM-XII 00202-2018). Infrastructural funding was provided by the ACCORD project co-financed by the European Regional Development Fund (ITMS2014+: 313021X329).

Appendix A. Supplementary data

Supplementary data to this article can be found online at https://doi.org/10.1016/j.ijpara.2024.04.007.

References

Bahia, A.C., Oliveira, J.H., Kubota, M.S., Araújo, H.R., Lima, J.B., Ríos-Velásquez, C.M., Lacerda, M.V., Oliveira, P.L., Traub-Csekö, Y.M., Pimenta, P.F., 2013. The role of reactive oxygen species in *Anopheles aquasalis* response to *Plasmodium vivax* infection. PLoS One 8, e57014.

Beneke, T., Demay, F., Hookway, E., Ashman, N., Jeffery, H., Smith, J., Valli, J., Bečvář, T., Myškova, J., Leštinová, T., Shafiq, S., Sádlová, J., Volf, P., Wheeler, R.J., Gluenz, E., 2019. Genetic dissection of a *Leishmania* flagellar proteome demonstrates requirement for directional motility in sand fly infections. PLoS Pathog 15, e1007828.

Beneke, T., Gluenz, E., 2019. LeishGEdit: a method for rapid gene knockout and tagging using CRISPR-Cas9. In: Clos, J. (Ed.), *Leishmania*. Humana Press, New York, NY, pp. 189–210.

Beneke, T., Madden, R., Makin, L., Valli, J., Sunter, J., Gluenz, E., 2017. A CRISPR Cas9 high-throughput genome editing toolkit for kinetoplastids. R Soc Open Sci 4, 170095.

Bianchi, C., Kostygov, A.Y., Kraeva, N., Záhonová, K., Horáková, E., Sobotka, R., Lukeš, J., Yurchenko, V., 2019. An enigmatic catalase of *Blastocrithidia*. Mol Biochem Parasitol 232, 111199.

Bienert, G.P., Møller, A.L., Kristiansen, K.A., Schulz, A., Møller, I.M., Schjoerring, J.K., Jahn, T.P., 2007. Specific aquaporins facilitate the diffusion of hydrogen peroxide across membranes. J Biol Chem 282, 1183–1192.

Brand, M.D., 2016. Mitochondrial generation of superoxide and hydrogen peroxide as the source of mitochondrial redox signaling. Free Radic Biol Med 100, 14–31.

Buchmeier, N.A., Libby, S.J., Xu, Y., Loewen, P.C., Switala, J., Guiney, D.G., Fang, F.C., 1995. DNA repair is more important than catalase for *Salmonella* virulence in mice. J Clin Invest 95, 1047–1053.

Burkard, G., Fragoso, C.M., Roditi, I., 2007. Highly efficient stable transformation of bloodstream forms of *Trypanosoma brucei*. Mol Biochem Parasitol 153, 220–223.

Butenko, A., Hammond, M., Field, M.C., Ginger, M.L., Yurchenko, V., Lukeš, J., 2021. Reductionist pathways for parasitism in euglenozoans? Expanded datasets provide new insights. Trends Parasitol 37, 100–116.

Carrero-Lérida, J., Pérez-Moreno, G., Castillo-Acosta, V.M., Ruiz-Pérez, L.M., González-Pacanowska, D., 2009. Intracellular location of the early steps of the isoprenoid biosynthetic pathway in the trypanosomatids *Leishmania major* and *Trypanosoma brucei*. Int J Parasitol 39, 307–314.

Chmelová, L., Bianchi, C., Albanaz, A.T.S., Režnarová, J., Wheeler, R., Kostygov, A.Y., Kraeva, N., Yurchenko, V., 2021. Comparative analysis of three trypanosomatid catalases of different origin. Antioxidants 11, 46.

Crowe, L.P., Morris, M.T., 2021. Glycosome heterogeneity in kinetoplastids. Biochem Soc Trans 49, 29–39.

Díaz, A., Loewen, P.C., Fita, I., Carpena, X., 2012. Thirty years of heme catalases structural biology. Arch Biochem Biophys 525, 102–110.

Diaz-Albiter, H., Sant'Anna, M.R., Genta, F.A., Dillon, R.J., 2012. Reactive oxygen species-mediated immunity against *Leishmania mexicana* and *Serratia marcescens* in the sand phlebotomine fly *Lutzomyia longipalpis*. J Biol Chem 287, 23995–24003.

Ding, M., Kwok, L.Y., Schluter, D., Clayton, C., Soldati, D., 2004. The antioxidant systems in *Toxoplasma gondii* and the role of cytosolic catalase in defence against oxidative injury. Mol Microbiol 51, 47–61.

Dubreuil, M.M., Morgens, D.W., Okumoto, K., Honsho, M., Contrepois, K., Lee-McMullen, B., Traber, G.M., Sood, R.S., Dixon, S.J., Snyder, M.P., Fujiki, Y., Bassik, M.C., 2020. Systematic identification of regulators of oxidative stress reveals non-canonical roles for peroxisomal import and the pentose phosphate pathway. Cell Rep 30 (1417–1433), e1417.

Dumas, A., Knaus, U.G., 2021. Raising the 'good' oxidants for immune protection. Front Immunol 12, 698042.

Edwards, C., Lloyd, D., 1977. Subcellular fractionation by differential and zonal centrifugation of the trypanosomatid *Crithidia fasciculata*. J Gen Microbiol 100, 339–346.

Freire, A.C.G., Alves, C.L., Goes, G.R., Resende, B.C., Moretti, N.S., Nunes, V.S., Aguiar, P.H.N., Tahara, E.B., Franco, G.R., Macedo, A.M., Pena, S.D.J., Gadelha, F.R., Guarneri, A.A., Schenkman, S., Vieira, L.Q., Machado, C.R., 2017. Catalase expression impairs oxidative stress-mediated signalling in *Trypanosoma cruzi*. Parasitology 144, 1498–1510.

Frolov, A.O., Kostygov, A.Y., Yurchenko, V., 2021. Development of monoxenous trypanosomatids and phytomonads in insects. Trends Parasitol 37, 538–551.

Fujiki, Y., Bassik, M.C., 2021. A new paradigm in catalase research. Trends Cell Biol 31, 148–151.

Ghosh, S., Banerjee, P., Sarkar, A., Datta, S., Chatterjee, M., 2012. Coinfection of *Leptomonas seymouri* and *Leishmania donovani* in Indian leishmaniasis. J Clin Microbiol 50, 2774–2778.

González-Flecha, B., Demple, B., 1995. Metabolic sources of hydrogen peroxide in aerobically growing *Escherichia coli*. J Biol Chem 270, 13681–13687.

Gould, S.J., Keller, G.A., Hosken, N., Wilkinson, J., Subramani, S., 1989. A conserved tripeptide sorts proteins to peroxisomes. J Cell Biol 108, 1657–1664.

Guy, B., Krell, T., Sanchez, V., Kennel, A., Manin, C., Sodoyer, R., 2005. Do Th1 or Th2 sequence motifs exist in proteins? Identification of amphipatic immunomodulatory domains in Helicobacter pylori catalase. Immunol Lett 96, 261–275.

Hamilton, P.T., Votýpka, J., Dostálová, A., Yurchenko, V., Bird, N.H., Lukeš, J., Lemaitre, B., Perlman, S.J., 2015. Infection dynamics and immune response in a newly described *Drosophila*-trypanosomatid association. mBio 6, e01356-01315.

Hart, D.T., Baudhuin, P., Opperdoes, F.R., de Duve, C., 1987. Biogenesis of the glycosome in *Trypanosoma brucei*: the synthesis, translocation and turnover of glycosomal polypeptides. EMBO J 6, 1403–1411.

Hewitt, O.H., Degnan, S.M., 2023. Antioxidant enzymes that target hydrogen peroxide are conserved across the animal kingdom, from sponges to mammals. Sci Rep 13, 2510.

Horáková, E., Faktorová, D., Kraeva, N., Kaur, B., Van Den Abbeele, J., Yurchenko, V., Lukeš, J., 2020. Catalase compromises the development of the insect and mammalian stages of *Trypanosoma brucei*. FEBS J 287, 964–977.

Ishemgulova, A., Kraeva, N., Faktorová, D., Podešvová, L., Lukeš, J., Yurchenko, V., 2016. T7 polymerase-driven transcription is downregulated in metacyclic promastigotes and amastigotes of *Leishmania mexicana*. Folia Parasitol 63, 016.

Ishemgulova, A., Kraeva, N., Hlaváčová, J., Zimmer, S.L., Butenko, A., Podešvová, L., Leštinová, T., Lukeš, J., Kostygov, A., Votýpka, J., Volf, P., Yurchenko, V., 2017. A putative ATP/GTP binding protein affects *Leishmania mexicana* growth in insect vectors and vertebrate hosts. PLoS Negl Trop Dis 11, e0005782.

Ishemgulova, A., Hlaváčová, J., Majerová, K., Butenko, A., Lukeš, J., Votýpka, J., Volf, P., Yurchenko, V., 2018. CRISPR/Cas9 in *Leishmania mexicana*: a case study of LmxBTN1. PLoS One 13, e0192723.

Izawa, S., Inoue, Y., Kimura, A., 1996. Importance of catalase in the adaptive response to hydrogen peroxide: analysis of acatalasaemic *Saccharomyces cerevisiae*. Biochem J 320, 61–67.

Joice, A.C., Lyda, T.L., Sayce, A.C., Verplaetse, E., Morris, M.T., Michels, P.A., Robinson, D.R., Morris, J.C., 2012. Extra-glycosomal localisation of *Trypanosoma brucei* hexokinase 2. Int J Parasitol 42, 401–409.

Kaasch, A.J., Joiner, K.A., 2000. Targeting and subcellular localization of *Toxoplasma gondii* catalase. Identification of peroxisomes in an apicomplexan parasite. J Biol Chem 275, 1112–1118.

Kato, N., Nelson, G., Lauersen, K.J., 2021. Subcellular localizations of catalase and exogenously added fatty acid in *Chlamydomonas reinhardtii*. Cells 10, 1940.

Khan, Y.A., Andrews, N.W., Mittra, B., 2018. ROS regulate differentiation of visceralizing *Leishmania* species into the virulent amastigote form. Parasitol Open 4, e19.

Kiaira, J.K., Njogu, R.M., 1983. Comparison of glycolysis in intact and digitonin-permeabilized bloodstream trypomastigotes of *Trypanosoma brucei*. Int J Biochem 15, 1379–1383.

Kostygov, A.Y., Albanaz, A.T.S., Butenko, A., Gerasimov, E.S., Lukeš, J., Yurchenko, V., 2024. Phylogenetic framework to explore trait evolution in Trypanosomatidae. Trends Parasitol 40, 96–99.

Kostygov, A.Y., Yurchenko, V., 2017. Revised classification of the subfamily Leishmaniinae (Trypanosomatidae). Folia Parasitol 64, 020.

Kovářová, J., Nagar, R., Faria, J., Ferguson, M.A.J., Barrett, M.P., Horn, D., 2018. Gluconeogenesis using glycerol as a substrate in bloodstream-form *Trypanosoma brucei*. PLoS Pathog 14, e1007475.

Kraeva, N., Ishemgulova, A., Lukeš, J., Yurchenko, V., 2014. Tetracycline-inducible gene expression system in *Leishmania mexicana*. Mol Biochem Parasitol 198, 11–13.

Kraeva, N., Butenko, A., Hlaváčová, J., Kostygov, A., Myšková, J., Grybchuk, D., Leštinová, T., Votýpka, J., Volf, P., Opperdoes, F., Flegontov, P., Lukeš, J., Yurchenko, V., 2015. *Leptomonas seymouri*: adaptations to the dixenous life cycle analyzed by genome sequencing, transcriptome profiling and co-infection with *Leishmania donovani*. PLoS Pathog 11, e1005127.

Kraeva, N., Horáková, E., Kostygov, A., Kořený, L., Butenko, A., Yurchenko, V., Lukeš, J., 2017. Catalase in Leishmaniinae: with me or against me? Infect Genet Evol 50, 121–127.

Kraeva, N., Leštinová, T., Ishemgulova, A., Majerová, K., Butenko, A., Vaselek, S., Bespyatykh, J., Charyyeva, A., Spitzová, T., Kostygov, A.Y., Lukeš, J., Volf, P., Votýpka, J., Yurchenko, V., 2019. *LmxM.22.0250*-encoded dual specificity protein/lipid phosphatase impairs *Leishmania mexicana* virulence *in vitro*. Pathogens 8, 241.

Kushnir, S., Gase, K., Breitling, R., Alexandrov, K., 2005. Development of an inducible protein expression system based on the protozoan host *Leishmania tarentolae*. Protein Expres Purif 42, 37–46.

Lefebre, M., Valvano, M., 2001. *In vitro* resistance of *Burkholderia cepacia* complex isolates to reactive oxygen species in relation to catalase and superoxide dismutase production. Microbiol-SGM 147, 97–109.

Lukeš, J., Butenko, A., Hashimi, H., Maslov, D.A., Votýpka, J., Yurchenko, V., 2018. Trypanosomatids are much more than just trypanosomes: clues from the expanded family tree. Trends Parasitol 34, 466–480.

Ma, M., Eaton, J.W., 1992. Multicellular oxidant defense in unicellular organisms. Proc Natl Acad Sci U S A 89, 7924–7928.

Manca, C., Paul, S., Barry, C.E.I., Freedman, V.H., Kaplan, G., 1999. *Mycobacterium tuberculosis* catalase and peroxidase activities and resistance to oxidative killing in human monocytes *in vitro*. Infect Immun 67, 74–79.

Mandell, G.L., 1975. Catalase, superoxide dismutase, and virulence of *Staphylococcus aureus*. *In vitro* and *in vivo* studies with emphasis on staphylococcal-leukocyte interaction. J Clin Invest 55, 561–566.

Merritt, C., Stuart, K., 2013. Identification of essential and non-essential protein kinases by a fusion PCR method for efficient production of transgenic *Trypanosoma brucei*. Mol Biochem Parasitol 190, 44–49.

Michels, P.A.M., Gualdrón-López, M., 2022. Biogenesis and metabolic homeostasis of trypanosomatid glycosomes: new insights and new questions. J Eukaryot Microbiol e12897.

Mikus, J., Steverding, D., 2000. A simple colorimetric method to screen drug cytotoxicity against *Leishmania* using the dye Alamar Blue. Parasitol Int 48, 265–269.

Mittra, B., Cortez, M., Haydock, A., Ramasamy, G., Myler, P.J., Andrews, N.W., 2013. Iron uptake controls the generation of *Leishmania* infective forms through regulation of ROS levels. J Exp Med 210, 401–416.
Monic, S.G., Lamy, A., Thonnus, M., Bizarra-Rebelo, T., Bringaud, F., Smith, T.K., Figueiredo, L.M., Rivière, L., 2022. A novel lipase with dual localisation in *Trypanosoma brucei*. Sci Rep 12, 4766.
Moraes, R.M., Freymuller, E., Camargo, E.P., Milder, R., 1994. Development of trypanosomatids in the phytophagous insect *Dysdercus peruvianus* (Hemiptera: Pyrrochoridae). A light and eletron microscopic study. Mem Inst Oswaldo Cruz 89, 553–559.
Neven, L.G., 2000. Physiological responses of insects to heat. Postharvest Biol Technol 21, 103–111.
Nicholls, P., Fita, I., Loewen, P.C., 2000. Enzymology and structure of catalases. Adv Inorg Chem 51, 51–106.
Nogueira, N.P., Saraiva, F.M., Sultano, P.E., Cunha, P.R., Laranja, G.A., Justo, G.A., Sabino, K.C., Coelho, M.G., Rossini, A., Atella, G.C., Paes, M.C., 2015. Proliferation and differentiation of *Trypanosoma cruzi* inside its vector have a new trigger: redox status. PLoS One 10, e0116712.
Okumoto, K., El Shermely, M., Natsui, M., Kosako, H., Natsuyama, R., Marutani, T., Fujiki, Y., 2020. The peroxisome counteracts oxidative stresses by suppressing catalase import *via* Pex14 phosphorylation. eLife 9, e55896.
Opperdoes, F.R., Butenko, A., Flegontov, P., Yurchenko, V., Lukeš, J., 2016. Comparative metabolism of free-living *Bodo saltans* and parasitic trypanosomatids. J Eukaryot Microbiol 63, 657–678.
Opperdoes, F.R., Michels, P.A., 1993. The glycosomes of the Kinetoplastida. Biochimie 75, 231–234.
Otera, H., Fujiki, Y., 2012. Pex5p imports folded tetrameric catalase by interaction with Pex13p. Traffic 13, 1364–1377.
Ouchi, Y., Unoura, K., Nabika, H., 2019. Role of oxidized lipids in permeation of H_2O_2 through a lipid membrane: molecular mechanism of an inhibitor to promoter switch. Sci Rep 9, 12497.
Penha, L.L., Sant'Anna, C.B., Mendonca-Previato, L., Cunha-e-Silva, N.L., Previato, J.O., Lima, A.P., 2009. Sorting of phosphoglucomutase to glycosomes in *Trypanosoma cruzi* is mediated by an internal domain. Glycobiology 19, 1462–1472.
Percy, M.E., 1984. Catalase: an old enzyme with a new role? Can J Biochem Cell Biol 62, 1006–1014.
Pyrih, J., Hammond, M., Alves, A., Dean, S., Sunter, J.D., Wheeler, R.J., Gull, K., Lukeš, J., 2023. Comprehensive sub-mitochondrial protein map of the parasitic protist *Trypanosoma brucei* defines critical features of organellar biology. Cell Rep 42, 113083.
Rhee, S.G., 1999. Redox signaling: hydrogen peroxide as intracellular messenger. Exp Mol Med 31, 53–59.
Sádlová, J., Podešvová, L., Bečvář, T., Bianchi, C., Gerasimov, E.S., Saura, A., Glanzová, K., Leštinová, T., Matveeva, N.S., Chmelová, L., Mlacovská, D., Spitzová, T., Vojtková, B., Volf, P., Yurchenko, V., Kraeva, N., 2021. Catalase impairs *Leishmania mexicana* development and virulence. Virulence 12, 852–867.
Schindelin, J., Arganda-Carreras, I., Frise, E., Kaynig, V., Longair, M., Pietzsch, T., Preibisch, S., Rueden, C., Saalfeld, S., Schmid, B., Tinevez, J.Y., White, D.J., Hartenstein, V., Eliceiri, K., Tomancak, P., Cardona, A., 2012. Fiji: an open-source platform for biological-image analysis. Nat Methods 9, 676–682.
Škodová, I., Verner, Z., Bringaud, F., Fabian, P., Lukeš, J., Horváth, A., 2013. Characterization of two mitochondrial flavin adenine dinucleotide-dependent glycerol-3-phosphate dehydrogenases in *Trypanosoma brucei*. Eukaryot Cell 12, 1664–1673.
Škodová-Sveráková, I., Záhonová, K., Bučková, B., Füssy, Z., Yurchenko, V., Lukeš, J., 2020. Catalase and ascorbate peroxidase in euglenozoan protists. Pathogens 9, 317.
Sollelis, L., Ghorbal, M., MacPherson, C.R., Martins, R.M., Kuk, N., Crobu, L., Bastien, P., Scherf, A., Lopez-Rubio, J.J., Sterkers, Y., 2015. First efficient CRISPR-Cas9-mediated genome editing in *Leishmania* parasites. Cell Microbiol 17, 1405–1412.
Souto-Padrón, T., de Souza, W., 1982. Fine structure and cytochemistry of peroxisomes (microbodies) *Leptomonas samueli*. Cell Tissue Res 222, 153–158.
Swinkels, B.W., Gibson, W.C., Osinga, K.A., Kramer, R., Veeneman, G.H., van Boom, J. H., Borst, P., 1986. Characterization of the gene for the microbody (glycosomal) triosephosphate isomerase of *Trypanosoma brucei*. EMBO J 5, 1291–1298.
Taub, J., Lau, J.F., Ma, C., Hahn, J.H., Hoque, R., Rothblatt, J., Chalfie, M., 1999. A cytosolic catalase is needed to extend adult lifespan in *C. elegans daf-C* and *clk-1* mutants. Nature 399, 162–166.
Thakur, L., Kushwaha, H.R., Negi, A., Jain, A., Jain, M., 2020. *Leptomonas seymouri* co-infection in cutaneous leishmaniasis cases caused by *Leishmania donovani* From Himachal Pradesh. India. Front Cell Infect Microbiol 10, 345.
Vercesi, A.E., Bernardes, C.F., Hoffmann, M.E., Gadelha, F.R., Docampo, R., 1991. Digitonin permeabilization does not affect mitochondrial function and allows the determination of the mitochondrial membrane potential of *Trypanosoma cruzi in situ*. J Biol Chem 266, 14431–14434.
Verplaetse, E., Rigden, D.J., Michels, P.A., 2009. Identification, characterization and essentiality of the unusual peroxin 13 from *Trypanosoma brucei*. Biochim Biophys Acta 1793, 516–527.
Villafraz, O., Biran, M., Pineda, E., Plazolles, N., Cahoreau, E., Ornitz Oliveira Souza, R., Thonnus, M., Allmann, S., Tetaud, E., Rivière, L., Silber, A.M., Barrett, M.P., Zíková, A., Boshart, M., Portais, J.C., Bringaud, F., 2021. Procyclic trypanosomes recycle glucose catabolites and TCA cycle intermediates to stimulate growth in the presence of physiological amounts of proline. PLoS Pathog 17, e1009204.
Virtanen, P., Gommers, R., Oliphant, T.E., Haberland, M., Reddy, T., Cournapeau, D., Burovski, E., Peterson, P., Weckesser, W., Bright, J., van der Walt, S.J., Brett, M., Wilson, J., Millman, K.J., Mayorov, N., Nelson, A.R.J., Jones, E., Kern, R., Larson, E., Carey, C.J., Polat, I., Feng, Y., Moore, E.W., VanderPlas, J., Laxalde, D., Perktold, J., Cimrman, R., Henriksen, I., Quintero, E.A., Harris, C.R., Archibald, A.M., Ribeiro, A. H., Pedregosa, F., van Mulbregt, P., SciPy, C., 2020. SciPy 1.0: fundamental algorithms for scientific computing in Python. Nat Methods 17, 261–272.
Wallace, F.G., 1977. *Leptomonas seymouri* sp. n. from the cotton stainer *Dysdercus suturellus*. J Protozool 24, 483–484.
Wang, Y.N., Wang, M., Field, M.C., 2010. *Trypanosoma brucei*: trypanosome-specific endoplasmic reticulum proteins involved in variant surface glycoprotein expression. Exp Parasitol 125, 208–221.
Xiang, L., Laranjeira-Silva, M.F., Maeda, F.Y., Hauzel, J., Andrews, N.W., Mittra, B., 2019. Ascorbate-dependent peroxidase (APX) from *Leishmania amazonensis* Is a reactive oxygen species-induced essential enzyme that regulates virulence. Infect Immun 87, e00193–00119.
Yurchenko, V., Votýpka, J., Tesařová, M., Klepetková, H., Kraeva, N., Jirků, M., Lukeš, J., 2014. Ultrastructure and molecular phylogeny of four new species of monoxenous trypanosomatids from flies (Diptera: Brachycera) with redefinition of the genus *Wallaceina*. Folia Parasitol 61, 97–112.
Yurchenko, V., Kostygov, A., Havlová, J., Grybchuk-Ieremenko, A., Ševčíková, T., Lukeš, J., Ševčík, J., Votýpka, J., 2016. Diversity of trypanosomatids in cockroaches and the description of *Herpetomonas tarakana* sp. n. J Eukaryot Microbiol 63, 198–209.
Zámocký, M., Furtmüller, P.G., Obinger, C., 2008. Evolution of catalases from bacteria to humans. Antioxid Redox Signal 10, 1527–1548.
Zámocký, M., Koller, F., 1999. Understanding the structure and function of catalases: clues from molecular evolution and *in vitro* mutagenesis. Prog Biophys Mol Biol 72, 19–66.
Zhong, M., Orosz, A., Wu, C., 1998. Direct sensing of heat and oxidation by *Drosophila* heat shock transcription factor. Mol Cell 2, 101–108.